EFDA–JET–PR(13)06

G. De Tommasi, A.C. Neto, F. Maviglia, P.J. Lomas, P. McCullen,
F. G. Rimini and JET EFDA contributors

Plasma Position and Current Control System Enhancements for the JET ITER-like Wall

Plasma Position and Current Control System Enhancements for the JET ITER-like Wall

G. De Tommasi[1], A.C. Neto[2], F. Maviglia[3], P.J. Lomas[4], P. McCullen[4], F.G. Rimini[4] and JET EFDA contributors*

JET-EFDA, Culham Science Centre, OX14 3DB, Abingdon, UK

[1]Associazione EURATOM-ENEA-CREATE, Univ. di Napoli Federico II, Via Claudio 21, 80125, Napoli, Italy
[2]Associazione EURATOM-IST, Instituto de Plasmas e Fusão Nuclear, IST, 1049-001, Lisboa, Portugal
[3]Associazione EURATOM-ENEA-CREATE, Via Claudio 21, 80125, Napoli, Italy
[4]EURATOM-CCFE Fusion Association, Culham Science Centre, OX14 3DB, Abingdon, OXON, UK
** See annex of F. Romanelli et al, "Overview of JET Results", (24th IAEA Fusion Energy Conference, San Diego, USA (2012)).*

Preprint of Paper to be submitted for publication in
Fusion Engineering and Design

ABSTRACT

The upgrade of Joint European Torus (JET) to a new all-metal wall, the so-called ITER-like wall (ILW), has posed a set of new challenges regarding both machine operation and protection. The Plasma Position and Current Control (PPCC) system plays a crucial role in minimizing the possibility that the plasma could permanently damage the ILW. The installation of the ILW has driven a number of upgrades of the two PPCC components, namely the Vertical Stabilization (VS) system and the Shape Controller (SC). The VS system has been enhanced in order to speed up its response and to withstand larger perturbations. The SC upgrade includes three new features: an improved termination management system, the Current Limit Avoidance system, and the PFX-on-early-task. This paper describes the PPCC upgrades listed above, focusing on the implementation issues and on the experimental results achieved during the 2011-12 JET experimental campaigns.

1. INTRODUCTION

The installation of the ITER-Like Wall (ILW) [1] has driven a number of upgrades to the JET Plasma Position and Current Control (PPCC) system. The overall design objective was the avoidance of overheating the ILW due to plasma thermal loads and hence the prevention of permanent damage to the wall surface. The PPCC system is composed of two subsystems, namely the Shape Control (SC) system, which regulates the plasma current and controls the plasma shape, and the Vertical Stabilization (VS) system that stabilizes the JET elongated plasmas.

The VS system was upgraded in 2009–10, before the ILWinstallation, and hence has been tested with the carbon wall, as part of the commissioning strategy, before use on the more fragile metal wall [2]. In particular, the system response has been sped up by increasing the maximum voltage of the radial field amplifier. The data acquisition has been replaced to increase the signal to noise ratio, and the processing capabilities have been increased to two gigaflops, allowing the execution of more complex control algorithms [3, 4]. The VS system can now withstand larger perturbations, e.g. larger Edge Localised Modes (ELMs). Furthermore, exploiting the flexibility and modularity of the VS real-time control system [5] which is based on the MARTe framework [6], it is possible:

- to execute different control algorithms, and scheduling them in order to maximize the performance in each plasma phase;
- to execute complex kick logic strategies with the possibility of also performing kicks with the divertor coils;
- to check and validate the whole real-time code (including both the control algorithm and the auxiliary code, i.e., communication interfaces with other systems, data acquisition, etc.) by using a plant model, before testing it on the plant.

A further package of activities was launched within the project Protection of the ITER-Like Wall (PIW) in 2011. Amongst these activities the SC was upgraded to include three new features: an improved termination management system, the Current Limit Avoidance system (CLA), and the

PFX-on-early-task (POET). Before these enhancements, one of the key problems for machine protection was that the termination of a pulse under fault conditions was limited to a predefined set of global responses, tailored for safe plasma landing or for reducing the vessel forces in case of plasma disruptions. Indeed, one of the possible force reduction strategies consists of pushing the plasma against the inner wall, which for the ILW, conflicts with the requirement that localised heat fluxes in the wall components should be avoided. The enhancement requires the update of several systems that are key to the machine operation, such as PPCC, the plasma density plant manager, and the additional heating systems. The new termination management system allows these subsystems (including PPCC) to dynamically adapt their responses according to the experimental conditions at the time of the stop request and during the termination itself. Such a solution is one of the first attempts to have a programmable pulse schedule (for two other examples, see [7] and [8]), which is one of the challenges for the ITER plasma control system [9]. The CLA avoids the current saturations in the poloidal field (PF) coils when the eXtreme Shape Controller is used to control the plasma shape. The CLA exploits the redundancy of the PF coils system to automatically obtain almost the same plasma shape using a different combination of currents in the PF coils, guaranteeing safer operation [10].

This paper deals with all these recent enhancements of the JET PPCC system, and also reports on some significant experimental results obtained during the first ITER-like wall campaigns at JET, in 2011–2012. The remainder of the paper is structured as follows: the next section gives a brief overview of the overall JET PPCC system. A detailed description of the recent enhancements for both the VS and SC, together with the relevant experimental results are presented in Section 3 and 4, respectively.

2. OVERVIEW OF THE JET PLASMA POSITION AND CURRENT CONTROL SYSTEM

This section gives an overview of the JET PPCC system. In particular, both the shape control and the vertical stabilization systems are presented. The end of this section briefly introduces the JET Level-1 system, which is the sophisticated JET pulse scheduling system that is responsible for translating the PPCC plant parameters into user-configuration variables and rules. For further details the reader can refer to [11] and [12].

The PPCC system is in charge of the axisymmetric magnetic control [13]. Indeed, when dealing with the control of the current, position and shape of the plasma column inside the vacuum vessel, the problem is typically considered axisymmetric, and the following three control issues are considered: the vertical stabilization, the plasma shape control, and the plasma current control.

On almost all existing machines, a frequency separation approach is adopted to solve the three aforementioned control problems. Following this approach, at JET the plasma is first vertically stabilized on a fast time scale, according to the constraints imposed by the passive structures and the actuator.

Afterwards, the current and shape controller is designed on the basis of the stable system obtained taking into account the vertical stabilization controller. In particular, for the JET tokamak, the time constant of the unstable mode is ~2ms, while the settling time of the current and shape controller is about 0.7s.

According to the frequency separation approach, the PPCC system has a distributed architecture which includes the two following subsystems

- the Vertical Stabilization (VS) system, which stabilizes the plasma by controlling the plasma vertical velocity;
- the Shape Control (SC) system, which controls both plasma current and shape (and hence also its position).

The VS and the SC systems are deployed on two different hardware platforms. In particular, the SC system runs with a 2ms cycle time on a ten years old VME board, which mounts a 400MHz PowerPCR CPU and executes the VxWorkstm OS. On the other hand, the VS system is deployed on a more recent ATCA/PCIe architecture, with a IntelR Core2Quad CPU that runs LinuxR -RTAI, with a cycle time of 50s.

These two heterogeneous hardware architectures are connected to the JET Real-Time Data Network (RTDN, [14]), which is a ATM/AAL5 communications on 155MHz fiber-optic. Each of the connected system sends application-specific datagrams into the network. For cross-platform interoperability, the datagrams have a fixed-size and structure, based on 32-bit integer or IEEE-754 floating point fields, with a simple header (sample number, sample time) and trailer (datagram version). The network switch distributes the datagrams to whichever system needs the information. Currently the JET RTDN connects more than 30 systems, exchanging 40 datagram types and a total of more than 500 signals.

As far as the real-time software is concerned the VS system has been developed using the MARTe framework [6], while the SC system exploits the MARTe's ancestor, called JETRT [15].

The actuators used by the PPCC system are the PF coils shown as red squares in Fig.1. These coils are linked together into 10 circuits, named P1, P4, IMB, SHA, PFX, D1, D2, D3, D4 and Radial Field circuit, each driven by independent power supplies. In particular, the P1 circuit is controlled by SC system and enables both the plasma inductive formation and the control of the plasma current. Furthermore, the SC system controls also P4, IMB, SHA, PFX, D1, D2, D3, and D4 to perform plasma shape control. The VS system stabilizes the plasma by controlling the current in the Radial Field circuit fed by the Radial Field Amplifier (RF A).

The block diagram in Fig.2 shows both the VS and SC systems. The VS system stabilizes the plasma column by controlling to zero its vertical velocity $\dot{z}_p(t)$. It tries also to minimize the control effort by controlling to zero the current flowing in the Radial Field circuit $I_{RFA}(t)$; furthermore keeping $I_{RFA}(t)$ small also allows the system to withstand bigger disturbances when they occur. Figure 2 depicts the internal structure of the SC system, showing its two main components, the Shape and

Plasma Current Controller and the PF Current Controller. The former computes the PF currents needed to counteract the disturbances and track the desired values for both the plasma current I_{Pref} (t) and of the plasma shape1. In the actual implementation of the SC system, the user can choose two different algorithms for plasma shape control:

- The standard Shape Controller [12], which is conceived as a solution to the shape control problem for the entire discharge. During the plasma formation process, this algorithms controls the currents in the PF circuits so that they track a set of preprogrammed waveforms. Afterward, when a small plasma column is formed, only the plasma radial position is controlled. Eventually, during the main experimental phase, i.e. when the plasma becomes bounded by a separatrix, the control is switched to the geometrical descriptors; in particular the standard Shape Controller gives the possibility of controlling simultaneously up to six geometrical descriptors.
- The eXtreme Shape Controller (XSC, [17, 18]), which can be used only after the separatrix formation. This algorithm permits to perform a more precise tracking of the overall plasma shape, by simultaneously controlling, in a mean square sense, more than 30 geometrical descriptors.

The PF Current Controller is designed to control the current in each PF circuit. In particular, it receives as input the references for the PF currents I_{ref} (t); these references are computed as the sum of two contributions:

- the feed-forward currents If f (t) (also called scenario currents), i.e. the PF currents needed to achieve the target reference in terms of plasma current and shape;
- the current requests computed by the Shape and Plasma Current Controller.

Based on the current control errors, the PF Current controller evaluates the voltages to be applied to the PF coils.

Note that both VS and SC systems generate voltage requests. Indeed in the case of VS, a current controller may introduce an unacceptable delay, limiting the system performances. On the other hand, the delay introduced by the PF Current Controller does not affect the overall behavior of the SC system, since this system reacts on a slower time scale with respect to the VS.

2.1. THE JET LEVEL 1

One of the most intricate issues of the JET PPCC system regards the setup and configuration of the different controllers. The configuration parameters can be separated in two distinct classes, one regarding plant expert settings (e.g. gains and protection limits) and another concerning the references requested by the experiment owner in order to achieve a given plasma state.

At JET the configuration of the different subsystems is performed using the so called Level-1 system. This provides a standardized user-interface

[1]The plasma shape is usually specified via a vector of geometrical descriptors $shape_{ref}$ (t) that includes gaps, strike points and X-point positions (see also Tutorial 7 in [16]).

where users can analyze, compare (e.g. against past experiments) and configure different plant parameters. It should be noticed that users with different roles will have different configuration permissions, depending on their expertise level and on the plant being updated.

The Level-1 system can also be considered as the first boundary machine protection, as it checks and limits the value of the parameters that are input in all the subsystems. However, it should be noted that neither PPCC nor Level-1 are protection systems and that JET has proper protection mechanisms that will stop the experiment in case of major problems in any of the relevant subsystems.

The PPCC system contains hundreds of expert parameters, associated both with the configuration of the controllers and with definition of the allowed operational windows. A large portion of these parameters are scalar values that do not vary with time, while others are setup as waveforms. The SC system and the Level-1 system share a common header file where all the configuration parameters are specified as C structures. After validating the user-input, and before the experiment, Level-1 marshals the configuration structure and sends a binary message to SC using a network protocol. Upon receipt of the message, SC decodes the configuration parameters and sets the plant accordingly.

In the VS system the configuration can be further divided in operational and experimental parameters. The former guarantee the vertical stabilization of the plasma throughout the experiment, while the latter enables the execution of experimental features associated with ELM pacing [19]. Taking advantage of the MARTe framework the configuration is sent by Level-1 directly in a text XML-like structure.

3. THE VERTICAL STABILIZATION SYSTEM

The VS system has been successfully upgraded within the Plasma Control Upgrade Project [20], which was closed out in summer 2010. The upgrade became necessary as JET prepared for more powerful experiments with the ILW, requiring the upgraded system to react extremely quickly to any vertical plasma movements, and to cope with different scenarios during the same experiment in a simple manner. To this aim the VS system flexibility has been increased, adding the capability of using different control algorithms during the discharge.

The system response time was improved by increasing the maximum voltage of the RF A [21], while the doubling of the maximum current increases the system capability of withstanding the largest disturbances. Furthermore, the data acquisition hardware was replaced to increase the signal to noise ratio [22], and the processing capabilities increased to two gigaflops, replacing the old controller based on four Texas Instruments DSPs [23] with a IntelR Core2Quad CPU; this gave the possibility of exploiting the modularity of the MARTe framework for the software development, allowing the deployment of more complex control algorithms (more details can be found in [5]).

3.1. IMPROVED PLASMA BREAKDOWN

The plasma formation is achieved in a tokamak fusion device by ionising the gas present in the toroidal vacuum chamber, with the application of a toroidal electric field. One important parameter

for the breakdown success is the initial electric field E0. The typical electric field of present tokamaks is about 1 V = m, while in the current ITER design it is limited to a value of about 0.33 V = m [24], leaving a lower margin for the breakdown success. Other important breakdown parameters are the toroidal magnetic field, and the poloidal magnetic stray field configuration. At JET the low electric field breakdowns have a higher occurrence of non sustained breakdown (NSB), which preclude the execution of some experiments and reduce precious experimental time. Moreover, at JET, during the early plasma phases it is diffcult to use magnetic measurements to control the evolution of the plasma column. Indeed, due to the typical small magnetic field values due to plasma at the breakdown, the magnetic measurements are strongly afected by noise, accuracy, number of effective bits and offsets, the latter due to the JET residual iron magnetization. ITER will have in addition further complications such as ferromagnetic inserts and vessel eddy currents which will have larger effects than in JET, as well as the fact that different amplifiers will be used to produce the primary transformer action, with a consequently higher synchronization precision required.

A finely tuned 2D FEM electromagnetic model, with a precision estimated to the order of a fraction of mT was employed to predict the stray field configuration during the JET breakdown and verified by the effect on the plasma starting position against the fast camera images [25]. This model includes the active PF circuits, a description of the passive structure and the JET magnetic circuit. The presence of an air-gap in the JET iron induces a perturbing field, with radial and vertical components, in the centre of the chamber. This perturbation is in the order of 0:5 mT during the breakdown phase. It turns out that the ideal hexapole magnetic null, which would be present in an up-down symmetric case, splits in two quadrupolar nulls in the direction of the perturbing field. In this condition the inboard lower null is expected to be preferred for plasma formation due to the higher electric and magnetic toroidal fields. In the breakdown phase of all past JET pulses the plasma was then pushed down in the divertor region by the radial field produced by the passive current flowing in the divertor conducting structures. Finally, for a successful breakdown the plasma was then pulled out by the vertical stabilization system, or terminated in the divertor region if the radial field circuit action was not suffcient.

An optimization was performed to correct the perturbing field by varying the radial field current over a range suggested by the calculation presented in [26]. The possibility of adding a bias for the radial field reference during breakdown was already present in the JET Level-1 interface and was already available with the old VS system, but it was never systematically exploited in order to optimize the plasma starting point formation. This was done in the 2011 experimental campaign by using the new VS system which inherited the possibility to introduce the designed radial field current corrections.

One feature revealed by these studies, and that had gone unnoticed since the installation of the new vertical stabilization system in 2009 [2, 27], was that the calibrated offsets of the data acquisition system measurements could slightly vary with a power cycle of the system. If the calibration curve was not readjusted a spurious offset would be introduced in the measurement and consequently

have an effect on the processed signals and on the feedback loop. As an example, an offset in the range of ±50 A (320 mV of ADC measurement with ± 32 V dynamic range) was sometimes present in the radial field current measurement, which translates to approximately to 0.2mT in the centre of the chamber. The presence of uncalibrated offsets was commonly linked to periods where low voltage breakdown were unreliable or even failed totally. Normal, higher voltage breakdown were usually unaffected. A 0.2mT offset can be considered small in terms of connection length and so stimulated further experimental studies at a lower electric field, i.e. $E_0 < 0.3V = m$. The precision required for the measurements in low electric field breakdown conditions may provide important information for the design of the acquisition system of machines with a limited E_0 value, i.e. ITER.

One of the advantages introduced with the new VS system is the higher speed of the system, due to the increase of the total maximum voltage from ±10kV to ±12kV, and to the lower inductance resulting from reduced P2R/P3R turns [2] (see Fig.1). This allows the system to react promptly in compensating the radial field produced by the passive structures situated in the lower in-vessel of the machine which support the divertor coils. Also the total time required for the full voltage swing from ~12kV to +12kV was reduced from the old to the new VS system, from 200s to 100s [20], respectively. Both these effects are considered to be very important to control the vertical position and speed of the nascent plasma in the very early stage, where the success of the breakdown is more fragile, and to avoid pushing the plasma down in the divertor region, where it usually ends up upon a failed attempt. Further safety margin was then introduced by the higher current limits, which passed from ±2.5kA to ±5kA and allows a larger clearance from the system limits during the breakdown, allowing a stronger controller action in case of need.

Since its introduction, the radial bias correction described above has been widely used and is currently applied in the vast majority of the experiments.

The new optimized plasma initial position avoids the plasma moving to the divertor region, and makes the breakdown more robust, with a lower occurrence of failed attempts. The new enhanced fast visible camera [28] has been used to validate the model prediction on plasma start-up and dynamic evolution. The optimized initial magnetic null position leads to an improved behaviour of the vertical stabilization system, with a smaller radial field current excursion, far from the amplifier limits (Fig.3). Thanks to the reoptimized breakdown recipe it has been possible to re-establish at JET a reliable low electric field “ITER like” breakdown down to $E_0 = 0.25$ V = m with the new beryllium wall and vertical stabilization system.

4. THE SHAPE CONTROL SYSTEM

Taking advantage of a large shutdown period for the installation of the new wall, it was decided also to perform a major upgrade of the shape controller software. The new system design was aimed at enabling the following features: a termination system that actively contributes to the protection of the ILW; the enabling of the flow of currents in the central solenoid which generate strong repulsive forces, allowing the pulse designer to greatly extend the amount of plasma time in configurations

of interest; and finally, a current limit avoidance algorithm that enables to fully exploit the XSC without risking to breach actuator limits. Each of these upgrades is justified and detailed in the following sections.

4.1. THE TERMINATIONS MANAGEMENT SYSTEM

The SC and VS plant settings are divided in a sequential list of timewindows in order to have an optimal set of settings for each experimental phase. The first time windows are reserved for the breakdown and plasma formation, and are followed by the development of the initial plasma shape. Once a stable plasma is achieved the SC can control many plasma shapes (each in its own time-window), as required by the specific scientific aims of each experimental pulse. At the end of the experiment a safe termination of the plasma is programmed via suitable choice of magnetic configuration and controlled ramp-down of the plasma current.

During the execution of the experiment it may become necessary to anticipate the termination of the plasma, either because a fault develops in another subsystem, the plasma becomes unstable, or a limit was reached in one of the actuators. To deal with such situations, the shape controller has six possible pre-programmed exit routes, the stops. For each of these, a control mode and a set of pre-programmed relative control references, usually scaled to the plant values and plasma state at the time of fault, is associated to each of the circuits controlled by SC. The stop to be executed is selected based on the type of fault triggered. Once the execution of a stop has started the time-windows are ignored until the end of the experiment.

The installation of the ITER-like wall highlighted some limitations in the previous PPCC SC stop strategy. The major problem was that the stop configuration did not explicitly depend on time, so that, for the same type of fault, the same stop response would be executed irrespectively of the experiment phase. These stop strategies could, potentially, lead to high localized heat fluxes in the wall components and hence thermal damage.

In order to deal with this issue, the SC system was updated [29], as part of the Protection of the ITER-like wall (PIW) project, so that the stop responses could be tailored for each time-window. Eight different stop responses, each associated with a different trigger, can now be specified for each plasma phase. A special type of stop, named jump-to-termination, enables the system to fast-forward to the plasma termination sequence. This can be very useful if the experiment is not performing as expected and allows one to anticipate the plasma termination following one of the properly commissioned plasma scenarios.

The PIWstops are triggered by the real-time protection sequencer (RTPS) [30], which acts as a central manager of all the PIW relevant diagnostics and actuators. These are sent to the SC system using the RTDN network. If the communication between RTPS and SC is lost for more than a configurable number of control cycles (typically 3, i.e. 6 ms), SC (or RTPS) will automatically trigger an original Pulse Termination Network (PTN) stop, i.e. a pre-PIW stop, and consequentially terminate the experiment. Amongst the most important inputs to RTPS are the measurements and

the processed signals coming from the Vessel Thermal Map (VTM) [31] system, which collects and monitors the temperature in several key regions of the vessel, and which is responsible for issuing an alarm to RTPS when any of the temperature limits is violated. In such cases RTPS will select the stop and send it to SC (and other subsystems) and consequently the plasma position and shape will likely be changed as a response to this event, e.g. to move away from a hot spot in the main chamber or divertor.

As shown in Fig. 4 the PTN stops are still available and are still useful for situations, such as coil protection alarms, where their proven robustness and reliability is more important than the requirement to protect the wall. In consequence, these stops have higher priority with respect to the PIW stops and can be triggered even after a PIW stop is in execution. The SC system allows for any number of PIW stops to be triggered while a PIW stop is already being executed. The stop configuration will always be the one associated with the time-window where the primary stop was issued.

Even if it is technically possible to trigger any number of stops, these are limited by RTPS, which constrains to a maximum of two in sequence. It should be noticed that with seven primary stops and six secondary it is already a challenge, while designing the pulse, to ensure that all possible paths are appropriate.

The length of the plasma pulses at JET is physically limited to a few tens of seconds, with a repetition rate that allows for between one and three pulses per hour. ITER plasma pulses are expected to last tens of minutes and eventually half an hour, so that if for any reason some of the required experimental resources are not available, it will be imperative to have at least one backup experimental plan [9]. Even for JET such a feature could greatly improve the scheduling of the experiments so that alternative experiments could still be executed after the beginning of the plasma pulse a given diagnostic or actuator is found not to be available.

In order to provide such a feature SC was upgraded to provide up to four alternative sequences. Each of the alternative sequences contains the same number of time-windows of the main sequence and contains its own stop response settings. The triggering of the alternative sequences would be performed by RTPS and implemented in the other plant managers in some future developments.

In order to assess the correct implementation of the PIW stopping logic an offine simulator, which executes the same code running in the plant, was developed and used with data from past experiments. All the possible stops, in different time-windows, were asserted using a unit-test algorithm that compared the outputs generated by simulator with the expected result. The stop triggering time, stop type and expected results were all configured as inputs to the unit-test.

The simulator was also tested against unlikely and forbidden requests, guaranteeing that even if triggered by an external entity to perform an invalid task, it still follows the correct path of action. An example of an invalid task could be: if RTPS were to request for a PIW stop to be triggered after a PTN stop was already being executed. Each simulation automatically generated a report that was used as part of the acceptance procedure for the PIW SC version. The software was subsequently installed in the plant and a series of integration tests and commissioning procedures were executed

in order to guarantee that the connection to RTPS was robust and that the real-time network link was performing with the required reliability.

After ensuring that the system still performed as in the pre-PIW stage (i.e. the same as with the previous version of the software) the correct response to the PIW stops was finally demonstrated using low-power technical plasmas, after which it was released for general use by the JET experimental programme.

Figure 5 shows the effect of a jump to termination on one of the SC controlled gaps. In the JET Pulse No: 80500 the plasma termination was expected to start after 25.8s of plasma. Driven by a thermal event at t = 20.204s the VTM system issued an alarm to RTPS, which was configured to trigger a jump to termination, when that particular event occurred in that specific timewindow.

After its release, the new termination system has been routinely used during the experimental campaigns, providing the first line of response when the plasma pulse deviates from the programmed experimental sequence. Taking into account only the plasma pulses that achieved a plasma current of at least 1.5MA, a total number of 2636 experiments were analyzed. From these, 669 plasma pulses (25.4%) had to be prematurely terminated.

From this subset of forced termination experiments, at the time of the stopping event, 470 (70.3%) were programmed to use as the primary mitigation strategy a PIWstop, being the remaining 199 (29.7%) being PTN stops. As shown in Fig.6 the events triggered by the magnetohydrodynamics mode activity (MHD), together with those driven by wall hotspots, account for the vast majority of primary PIW stops. As expected, the jump to termination was also routinely used as the preferred primary exiting strategy. Defining a successful stop as a termination that manages to drive the plasma current to a value of less than 1MA, without triggering any subsequent stop, 249 (53%) of the PIW primary stops successfully terminated the plasma pulse.

When the primary stop fails to mitigate the event which triggered the termination, or the stopping strategy itself generates a higher priority termination event, then a secondary stop is started. The total number of secondary stops that had to be triggered was 420, of which 111 (22 %) were programmed to be a PIW stop. There are two main reasons for the decrease in the number of PIW secondary selected stops: (i) a PIW stop can never preempt a PTN stop, so that any primary PTN stop can never be followed by a PIW secondary; (ii) upon the failure of a primary PIW stop, machine operators prefer to try to land the plasma using a strategy that has a demonstrated track record. As depicted in Fig. 7, the two main exceptions to these cases are the PIW secondary related to MHD driven stops, since these are specially designed to handle events where it is the PIW primary stop that generates a higher priority plasma termination event. The number of successful pulses that was terminated with a secondary stop was 54 (48.6%), so that the total (primary and secondary) percentage of PIW successfully terminated pulses was 64.6%.

4.2. POET

The JET central solenoid, the P1 circuit, is composed of 10 pancakes, all fed in series by a Flywheel Generator (PF-FGC). In addition, a separate two-quadrant amplifier, denoted as PFX, feeds the six

central pancakes to obtain highly shaped magnetic configurations, including those characterised by a magnetic X-point inside the vacuum vessel. The six central pancakes are denoted as P 1C, while the remaining two upper and two lower are known as P 1E . In order to avoid damage due to repulsive vertical forces between central and external pancakes when current is flowing in opposite directions, forces which are balanced only by the net weight of the upper part of the JET structure, severe limitations have always been imposed on the operation of PFX in the early phases of the pulse, when the P1E current is negative or close to zero. More specifically, before POET was put in operation, it was possible to energize the PFX circuit only when the PF-FGC current (see Fig.8) was already in the same direction as the PFX current and greater than a prescribed positive value, usually set to 3kA. This requirement posed a significant constraint on how early certain magnetic configurations, e.g. the X-point equilibria, could be achieved in a plasma pulse.

In order to anticipate the time at which current is allowed in the PFX circuit and hence to expand the X-point operational window, a modelling activity was carried out to provide a more accurate estimation of the ejection forces acting on the upper coils and to compare them with the more recent limits for the total weight of the upper machine. A detailed discussion about the modelling activity is given in [32]. For this task the 2D CREATE [33] and ANSYS electromagnetic models of the JET machine, both including a non linear B–H characteristic of the iron, have been compared and validated. A series of static reconstructions have been run in order to assess all the force contributions acting on the components of interest of the magnetic and electric circuits. The analysis indicated that plasmaless conditions generate higher ejection forces than with plasma: the plasmaless case has, therefore been set as the reference force map with a safe limit set 3 MN. This choice implies that the case of a possible sudden loss the plasma during a disruption event is fully included in the safety considerations.

The POET system has been implemented taking into account the following constraints:

- the upgrade shall not imply any changes to the present PPCC hardware;
- the upgrade shall be designed within the existing software framework and shall minimize the changes to the code.

The main reasons were that the changes could not jeopardize the present P1 protection logic and had to maintain the existing capability of operating PPCC for negative and positive plasma current. Thanks to its modularity, the SC system contains a well defined and separated C++ module devoted to all the logic concerning the P1 circuit. This logic is based on an internal state machine, that can be changed either by an hardware event or by a software internal transition. The former can only occur when a Central Timing and Trigger System (CTTS) state change is detected, while the latter is based on a series of checks on the P1E and PFX current values. If one of the P1 limits is reached, SC will trigger a PTN slow stop. All the limits related to P1 can be set using the SC expert Level-1 interface. The previous logic included a unique limit, named IP1E LOWER LIMIT, which could assume only non-negative values, and was typically set to 3kA. Operation of the PFX circuit was

only enabled once the P1E current was larger than the IP1E LOWER LIMIT. In the new logic the value of IP1E LOWER LIMIT can be negative, typically –2kA, and an additional restriction is imposed on the absolute value of PFX current, typically 7–9kA, when I P 1E is lower than the IP1E LOWER LIMIT.

After the introduction of the POET mode in SC, the system was first tested offine, focusing on a thorough assessment of the new logic and overall behavior of the system in a large variety of realistic operational scenarios. As previously stated the SC is not a protection system, although it represents the first line of defence against off-normal events and potentially dangerous operation. The two independent JET coil protection systems, the software Coil Protection System (CPS) and the hardwired Ohmic Heating Measurement and Protection Cubicle (OH-MPC) have current limits progressively higher than the Shape Control settings and have been modified to accommodate the POET operational space.

After the successfully commissioning completed at the start of the 2011 ITER-like wall exploitation, the POET feature has been routinely used allowing for an optimized operation of the machine. Positive results have been achieved in the anticipation of the X-point formation by ~5s, and in increasing the duration of relevant operational scenarios and allowing the earlier achievement of the desired final configurations (see Fig.9).

4.3. CURRENT LIMIT AVOIDANCE SYSTEM

This section briefly describes the CLA system, which implements the current allocation algorithm described in [10] to avoid current saturations in the PF coils when the XSC is used to control the plasma shape. The XSC minimizes a quadratic cost function of the plasma shape error in order to obtain, at the steady state, the output that best approximates the desired shape. Thanks to the XSC, the pulse designers can directly specify the target shape, without specifying the PF current waveforms (see Section V in [34]), which are automatically computed by model-based control algorithm. The XSC algorithm, however, does not take into account the current limits in the PF coils and may produce PF current request outside the permitted ranges. The CLA has been implemented to solve this problem, allowing the use of the XSC even when the PF currents are close to their saturation values.

The CLA algorithm aims at keeping the PF currents within their limits without degrading too much the plasma shape, by finding an optimal trade–off between these two objectives (more details can be found in [10]). In particular, the CLA modifies the PF current requests computed by the XSC before sending them to the PF current controller. Fig. 10 shows a block diagram of the JET shape controller as it has been modified in order to deploy the CLA system. In particular, the CLA system receives as inputs:

1. the PF current requests computed by the XSC;
2. the reference shape for the XSC (gaps, strike-points and X-point position);
3. the shape measurements (gaps, strike-points and X-point position).

and gives as outputs:

1. the modified PF currents requests to be sent to the PF currents controller;
2. the additional references (gaps, strike-points, and X-point position) to be sent back to the XSC, in order to hide the plasma shape variation induced by the CLA.

Thanks to the modularity of the JETRT framework (which is in some regard very similar to its successor MARTe), the CLA block depicted in Fig.10 has been implemented as an independent and isolated plug-in; this has significantly facilitated the test and validation phase, reducing to the minimum the operational time required for commissioning on the real plant.

In particular, the JET commissioning procedure for the CLA involves the simulation of the two saturation levels in the 8 PF circuits used by the XSC. The simulation of the saturation is obtained by changing the corresponding CLA limits.

Figure 11 shows the currents in the PF coils for the commissioning Pulse No: 81079, during which the lower limit for the D4 current was tested. In particular, the limit was set equal to 4:5 kA and the CLA was switched on at t = 25 s. It can be noticed that at steady state the current in D4 reaches the desired value, while the other PF currents slightly change in order to keep the plasma shape, as shown in Fig. 12.

Further on, during the commissioning pulse #81081, the lower limit for the P4 current was set equal to 7kA, but the CLA was not able to enforce the desired value, as shown in Fig. 13. Indeed in this case, the error on the plasma shape due to the P 4 current change is not negligible as it is shown in Fig.14; this behavior was the expected one for the chosen CLA parameters and it was also reproduced in simulation by using the XSC Tools [35].

After the commissioning phase, an experiment has been carried out in early 2012, which was aimed at producing a severe limitation for the plasma shape control, and hence to prove the effectiveness of the CLA system. In order to do that, up to four out of the eight PF currents available for plasma shape control have been limited.

The following strategy has been adopted to carry out the experiment; first the reference pulse was run (Pulse No: 81710), where the XSC without CLA has successfully controlled the plasma shape between 20s and 23s.

Afterwards, during the Pulse No: 81715, the CLA has been then enabled from 21s, in order to limit the currents in the four divertor coils D1–D4 within a range smaller than the one actually available. In particular, the following ranges have been considered: ID1 has been limited within [–16.5; –4] kA, ID2 in [–31.5 ;–10] kA, while ID 3 and ID 4 have been limited between [–11 ;–2] kA and [0.6] kA, respectively.

As expected, when a PF current is outside its saturation limits, the CLA tries to bring it back in the permitted range while obtaining almost the same plasma shape as shown in Fig. 15. Moreover, Fig.16 shows a comparison between the divertor currents for Pulse No's: 81710 and 81715. Taking into account that the limitation of more than two control currents represents already a challenging scenario for the CLA, the performance obtained during the Pulse No: 81715 is considered fully satisfactory. Furthermore, it is important to note that the CLA parameters used in the considered

experiment included a hard constraint on the X-point position. Indeed, when computing the new equilibrium currents, the CLA prefers to increase the shape error on the top-outer region of the plasma, rather than to change the position of the X-point, as shown in Fig. 15.

Thanks to CLA, plasma operations have been made safer, and the session leaders have gained more confidence in using the XSC. As an example, although the XSC is available at JET since 2003, in 2012 the pulse #83014 has been the first pulse ever to be controlled with XSC soon after the Xpoint formation, up to the plasma termination. Thanks to the CLA, it has been possible to exploit the XSC in order to better control the plasma shape during both the plasma current ramp-up and ramp-down, when some PF currents are close to their saturation limits [36].

CONCLUSIONS

The JET PPCC was upgraded in order to cope with the operational requirements of the ILW. The flexibility of the new VS architecture has been exploited to improve the breakdown phase, while the overall system upgrade has increased the capability of rejecting large disturbances. Furthermore, two new features have been added to the SC, mainly aimed at minimizing the possibility that the plasma thermally overloads the ILW. In particular, a new stopping architecture enables a greater control over the experiment and enhances the first line of defence for the machine protection. The CLA aids safe operations when using the XSC to control the plasma shape, since it prevents the control algorithm from requesting currents in the PF coils that are outside the permitted range. Finally, a new operational mode, named POET, enables an earlier exploitation of the X-point configuration, optimising experimental resources and time.

ACKNOWLEDGMENTS

This work was supported by EURATOM and carried out within the framework of the European Fusion Development Agreement. The views and opinions expressed herein do not necessarily reflect those of the European Commission. The authors would like to thank John Last, Valeria Riccardo, Stephen Shaw and Paul Smith for their contribution to the POET system, Giuseppe Ambrosino, Alfredo Pironti, Gianluca Varano, Riccardo Vitelli and Luca Zaccarian for their contribution to the implementation of the CLA, Raffaele Albanese and Massimiliano Mattei for their support to the modeling activities and, finally, Ana Manzanares for the data of the JET fast camera shown in Fig. 3.

REFERENCES

[1]. G. Matthews, et al., JET ITER-like walloverview and experimental programme, Physica Scripta 2011 (T145) (2011) 014001. URL http://stacks.iop.org/1402-4896/2011/i=T145/a=014001

[2]. F. Rimini, et al., First plasma operation of the enhanced JET vertical stabilisation system, Fusion Engineering and Design **86** (6–8) (2011) 539–543.

[3]. F. Sartori, et al., The PCU JET Plasma Vertical Stabilization control system, Fusion Engineering and Design **85** (3–4) (2010) 438–442.

[4]. A. Neto, et al., Exploitation of Modularity in the JET Tokamak Vertical Stabilization System, Control Engineering Practice **20** (9) (2012) 846–856.

[5]. T. Bellizio, et al., The Software Architecture of the New Verical Stabilization System for the JET tokamak, IEEE transactions on plasma science **38** (9) (2010) 2465–2473.

[6]. A. Neto, et al., MARTe: a Multi-platfrom Real-time Framework, IEEE Transactions on Nuclear Science **57** (2) (2010) 479–486.

[7]. G. Neu, et al., The ASDEX Upgrade discharge schedule, Fusion Engineering and Design **82** (5–14) (2007) 1111–1116.

[8]. P. Moreau, et al., Failure mode and recovery strategies for the operation of the Tore Supra tokamak, in: Proc. 12th Int. Conf. on Accelerator and Large Experimental Physics Control Systems (ICALEPCS'09), Kobe, Japan, 2009, pp. 591–593.

[9]. G. Raupp, et al., Real-time exception handling – Use cases and response requirements, Fusion Engineering and Design **87** (12) (2012) 1891–1894.

[10]. G. De Tommasi, et al., Nonlinear dynamic allocator for optimal input/ output performance trade-off: application to the JET Tokamak shape controller, Automatica 47 (5) (2011) 981–987.

[11]. M. Lennholm, et al., Plasma control at JET, Fusion Engineering and Design **48** (1–2) (2000) 37–45.

[12]. F. Sartori, G. De Tommasi, F. Piccolo, The Joint European Torus, IEEE Control Systems Magazine **26** (2) (2006) 64–78.

[13]. G. De Tommasi, et al., Current, position, and shape control in tokamaks, Fusion Science Technology **59** (3) (2011) 486–498.

[14]. R. Felton, et al., Real-time plasma control at JET using ATM network, in: Proc. 11th IEEE NPSS Real Time Conference, Santa Fe, New Mexico, 1999, pp. 175–181.

[15]. G. De Tommasi, F. Piccolo, A. Pironti, F. Sartori, A flexible software for real-time control in nuclear fusion experiments, Control Engineering Practice **14** (11) (2006) 1387–1393.

[16]. A. Beghi, A. Cenedese, Advances in Real-Time Plasma Boundary Reconstruction, IEEE Control Systems Magazine **25** (5) (2005) 44–64.

[17]. M. Ariola, A. Pironti, The design of the eXtreme Shape Controller for the JET tokamak, IEEE Control Systems Magazine **25** (5) (2005) 65–75.

[18]. G. Ambrosino, M. Ariola, A. Pironti, F. Sartori, Design and implementation of an output regulation controller for the JET tokamak, IEEE Transactions on Control Systems Technology **16** (6) (2008) 1101–1111.

[19]. F. Sartori, P. Lomas, F. Piccolo, M. Zedda, Synchronous ELM pacing at JET using the Vertical Stabilisation controller, in: Proc. 35th EPS Conference on Plasma Physics, 2008, pp. P–5.045.

[20]. F. Sartori, et al., The JET PCU project: an international plasma control project, Fusion Engineering and Design **83** (2–3) (2008) 202–206.

[21]. D. Ganuza, et al., The design and manufacture of the enhanced radial field amplifier (ERFA) for the JET project, Fusion Engineering and Design **84** (2–6) (2009) 810–814.

[22]. A. J. N. Batista, et al., ATCA Control System Hardware for the Plasma Vertical Stabilization in the JET Tokamak, IEEE Transactions on Nuclear Science **57** (2) (2010) 583–588.

[23]. M. Garribba, et al., First operational experience with the new plasma position and current control system of JET, in: Proc. 18th Symposium of Fusion Technol., Karlsruhe, 1994, pp. 747–750.

[24]. A. Sips, et al., Experimental studies of ITER demonstration discharges, Nuclear Fusion **49** (8) (2009) 085015.

[25]. F. Maviglia, et al., Electromagnetic analysis of breakdown conditions in JET, Fusion Engineering and Design **86** (6–8) (2011) 675–679.

[26]. R. Albanese, et al., Experimental results with an optimized magnetic field configuration for JET breakdown, Nuclear Fusion **52** (12) (2012) 123010.

[27]. R. Albanese, et al., Overview of modelling activities for Plasma Control Upgrade in JET, Fusion Engineering and Design **86** (6–8) (2011) 1030–1033.

[28]. E. de la Cal, et al., The Visible Intensified Fast Camera with Wide- Angle View of JET ITER-Like Wall Experiment, in: Proc. 39th EPS Conf. on Plasma Phys., Stockholm, Sweden, 2007.

[29]. A. Neto, et al., Shape Controller Upgrades for the JET ITER-like Wall, in: 13th International Conference on Accelerator and Large Experimental Physics Control Systems (ICALEPCS'11), 2011. URL http://www.esrf.eu/icalepcs2011/papers/mopmu035.pdf

[30]. A. Stephen, et al., Centralised Coordinated Control to Protect the JET ITER-like Wall, in: 13th International Conference on Accelerator and Large Experimental Physics Control Systems (ICALEPCS'11), 2011. URL http://www.esrf.eu/icalepcs2011/papers/fraault04.pdf

[31]. D. Alves, et al., Vessel thermal map real-time system for the JET tokamak, Phys. Rev. STAccel. Beams 15 (2012) 054701. doi:10.1103/PhysRevSTAB.15.054701. URL http://link.aps org/doi/10.1103/PhysRevSTAB.15.054701

[32]. F. Maviglia, et al., JET modeling and control analysis for POET (PFX Operating Early Task), Fusion Engineering and Design doi: 10.1016/j.fusengdes.2013.02.054.

[33]. R. Albanese, F. Villone, The linearized CREATE-L plasma response model for the control of current, position and shape in tokamaks, Nuclear Fusion **38** (5) (1998) 723–738.

[34]. G. De Tommasi, et al., XSC Tools: a software suite for tokamak plasma shape control design and validation,IEEE Transactions on Plasma Science **35** (3) (2007) 709–723.

[35]. G. De Tommasi, et al., A Software Tool for the Design of the Current Limit Avoidance System at the JET Tokamak, IEEE Transactions on Plasma Science **40** (8) (2012) 2056–2064.

[36]. G. Calabró, et al., H-mode and L-H threshold experiments during ITERlike plasma current ramp up/down at JET with ILW, in: 40th EPS conference on Plasma Physics, Espoo, Finland, 2013.

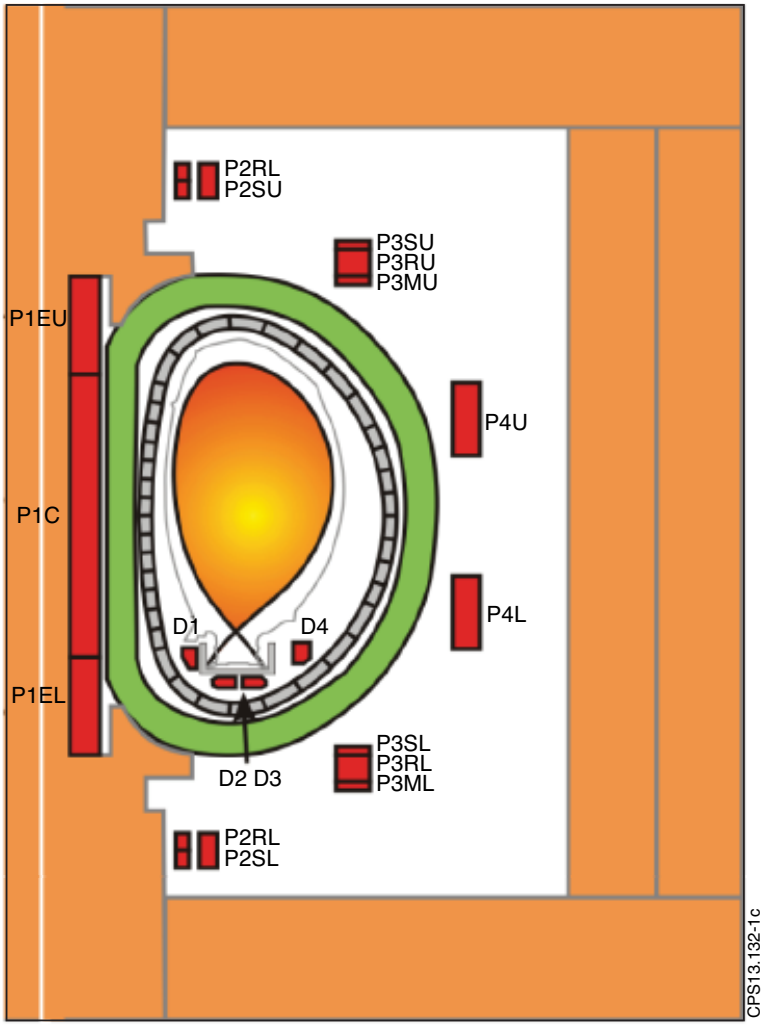

Figure 1: The JET poloidal field coils system. The radial field circuit connects the P2RU, P3RU, P2RL, and P3RL, and is fed by the Radial Field Amplifier (RFA). This amplifier is used by the VS system to vertically stabilize the plasma column. The P1 circuit includes the elements of the central solenoid P1EU, P1C, P1EL, as well as P3MU and P3ML. The series circuit of P4U and P4L is named P4, while the circuit that creates an imbalance current between the two coils is referred to as IMB. SHA is made of the series circuit of P2SU, P3SU, P2SL, and P3SL. The central part of the central solenoid contains an additional circuit named PFX. Finally the four divertor coils (D1 to D4) are driven separately each by one power supply

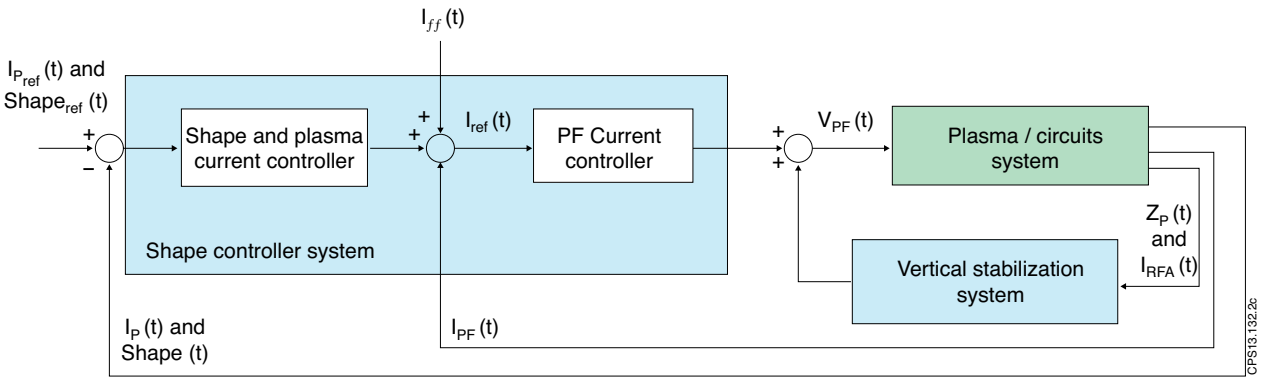

Figure 2: Simplified block diagram of the JET PPCC system.

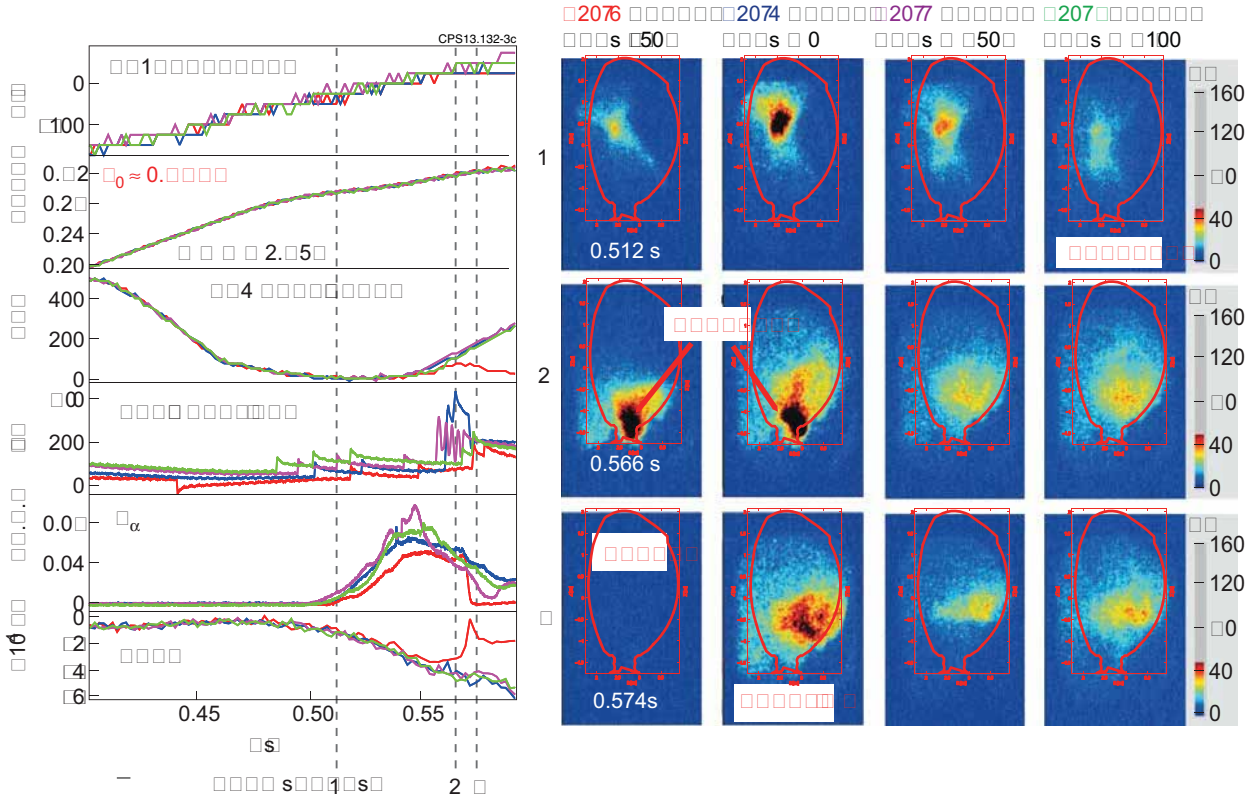

Figure 3: Experimental data and images from the JET fast visible camera for a radial bias scan with initial primary current $I_{P1} \sim 0$. The vertical dashed lines in the experimental plots indicate the time where the pictures are captured. In the plots on the left are shown the primary current, the electric field at r = 2.95m, the vertical and radial field currents. In the last two plots are shown one of the H-alpha emission lines, and the plasma current evolutions.

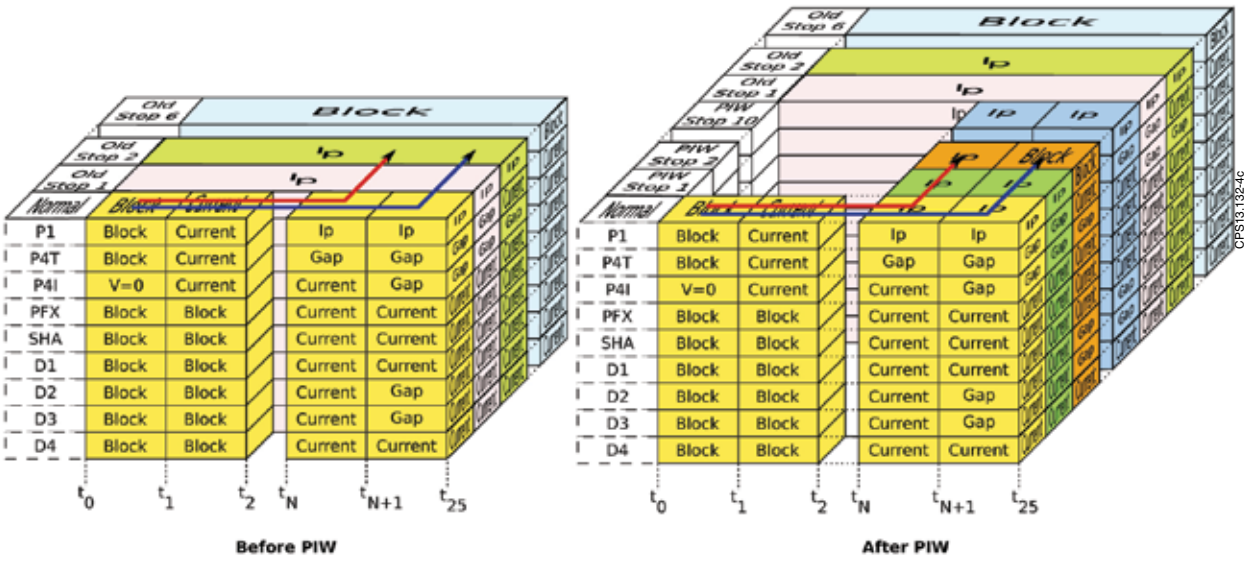

Figure 4: The new stopping strategy developed for the ITER-like wall allows stopping strategies tailored for each of the plasma phases. These allow the configuration of different control modes and control references for each of the SC time windows or to anticipate the end of the experiment by following the optimal plasma landing recipe. As shown in this figure, before the PIW, when a given stop was triggered the control strategy was the same irrespective of the stopping trigger time. As an example, when the "Old Stop 2" was triggered the P1 control mode would always be IP. After the PIW, the new stops are allowed to have a different control mode for each of the available time windows. For example, if PIW stop 2 is triggered between t_N and t_{N+1} the P1 control mode will be IP, but if it is triggered between t_{N+1} and t25 the P1 control mode will be BLOCK.

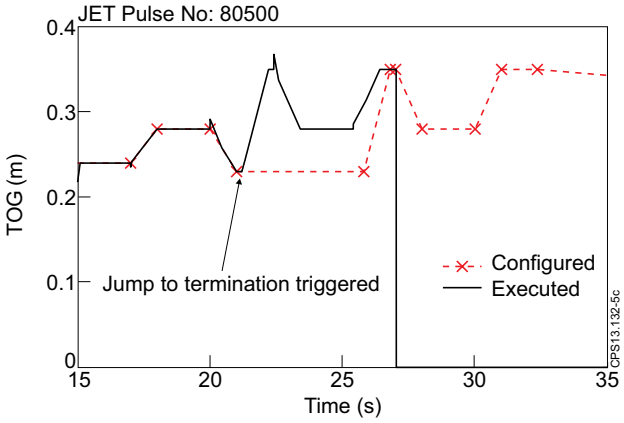

Figure 5: In the JET Pulse No: 80500 the plasma termination was expected to start at t = 25.8s. Due to an thermal driven event a jump to termination was triggered at t = 20.204s. This figure depicts the control reference for one of the gaps being controlled by SC, named Top Gap (TOG), and it shows the anticipation of the control reference to the time of the jump to termination event.

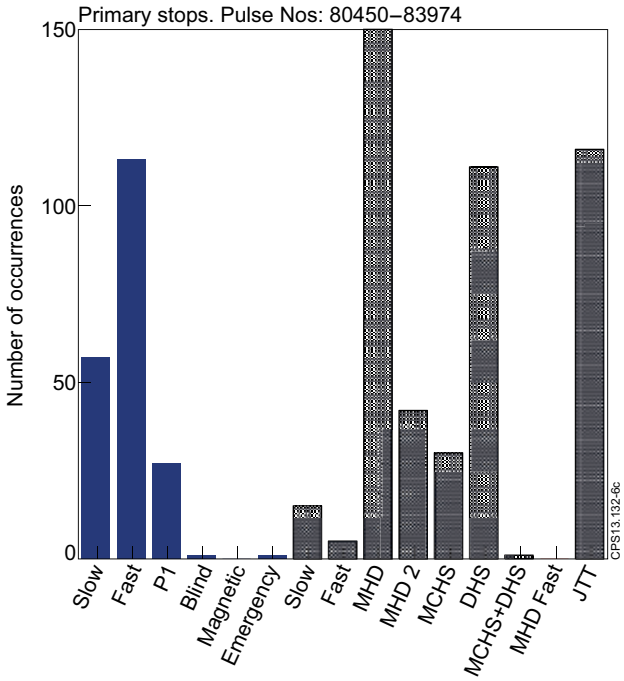

Figure 6: Number of occurrences for each termination type since the PIW stops are available. The squared pattern represents the new PIW stops while the filled pattern shows the stops that were already available before the update. MHD are the magnetohydrodynamics instabilities driven stops, while the MCHS and DHS are the main chamber and divertor hot spot triggered terminations. The vast majority of the plasma terminations are already based on strategies that take advantage of the new PIW stops, allowing MHD instabilities and hotspots to be handled with more discrimination. The jump to termination (JTT) was also used a large number of times as the most appropriate way to terminate the plasma.

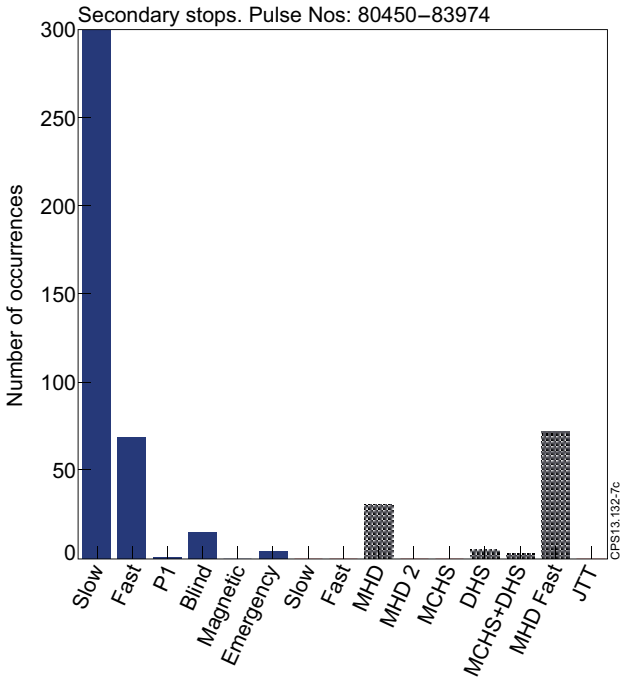

Figure 7: The secondary stops are triggered upon the failure of the primary stop to mitigate the termination driving event. The preferred secondary plasma stop is the PTN slow stop. MHD fast events are some times created by the primary stop plasma mitigation so that this plasma termination is usually only used as a secondary stop strategy.

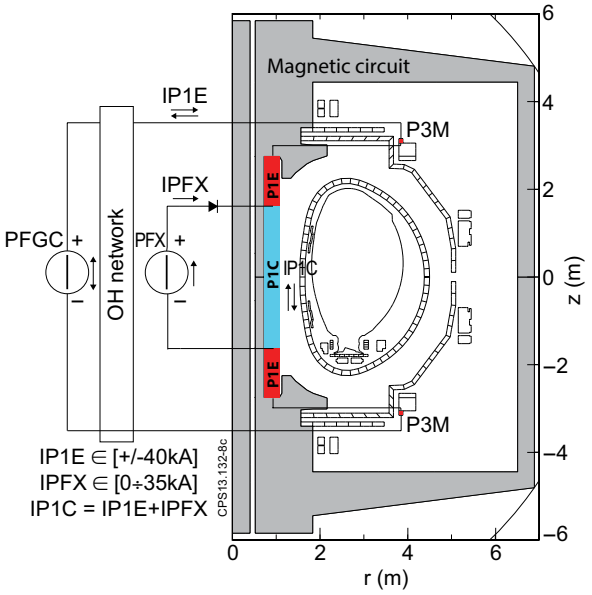

Figure 8: The Poloidal Flywheel Generator Converter (PFGC) feeds the whole primary circuit (more details on this power converter can be found in [12]), while the PFX amplifier only feeds the central pancakes of the central stack. The model of the considered magnetic circuit is highlighted in grey.

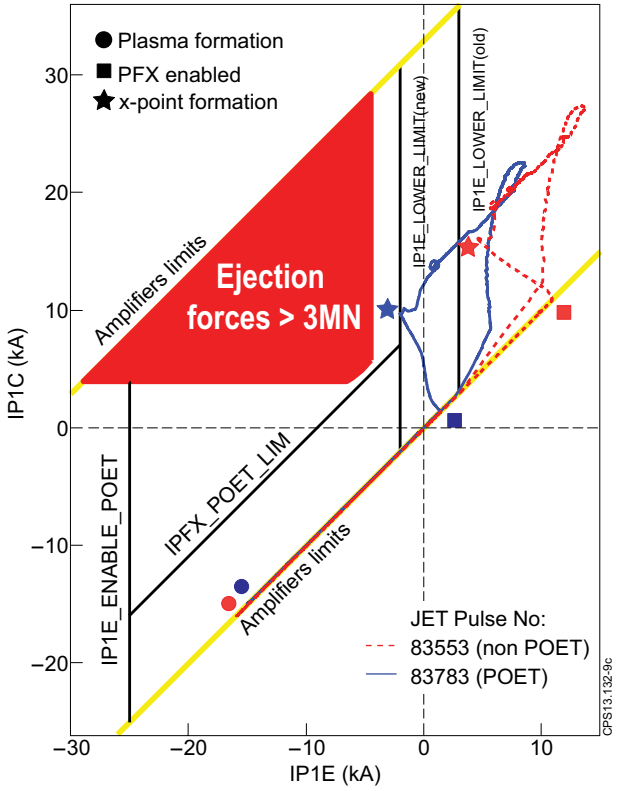

Figure 9: POET logic implementation superimposed on experimental Pulse No: 83553 (dashed), and a POET Pulse no: 83783 (solid) traces. In the latter the IP1E LOWER LIMIT was set to –2kA and it was possible to anticipate the X-point formation by ≅5s.

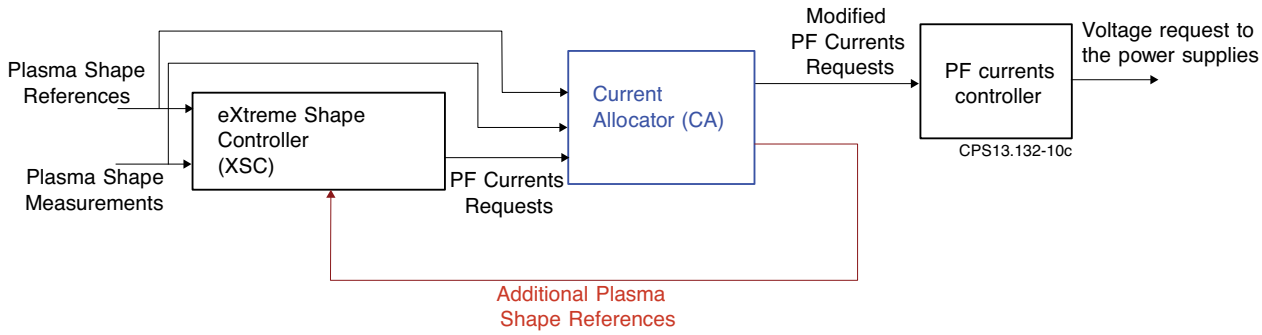

Figure 10: Block diagram of the Shape Controller system, including the XSC and the CLA.

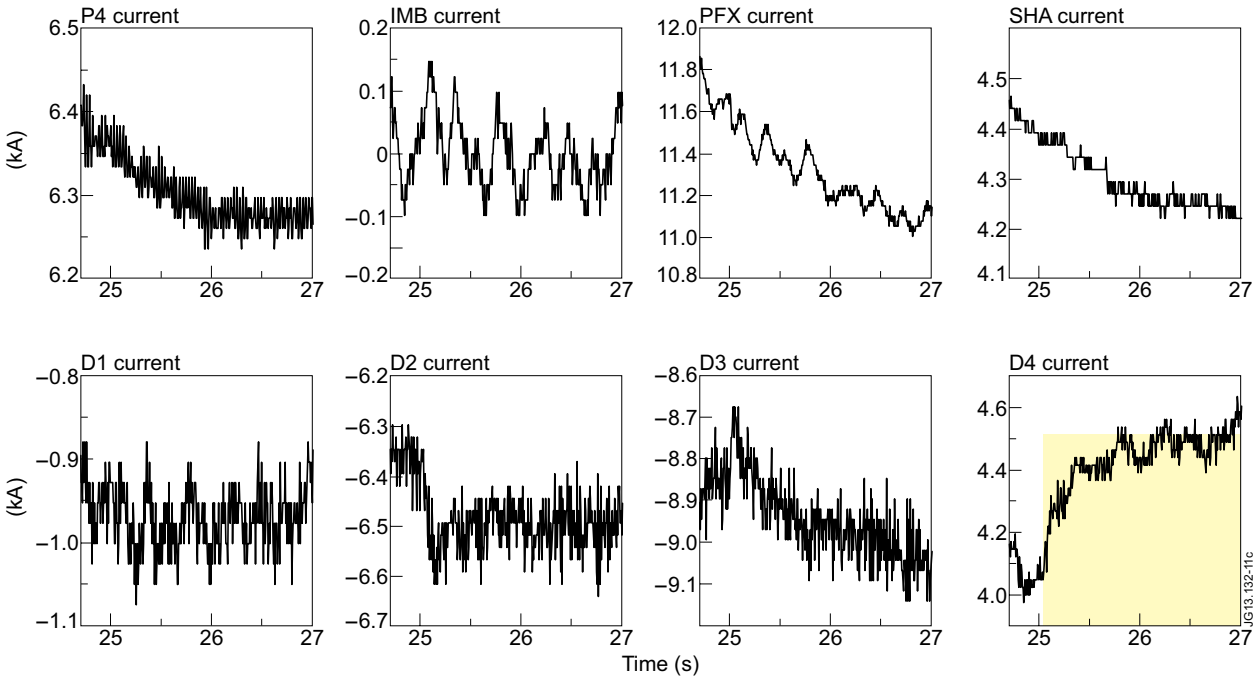

Figure 11: Currents in the PF coils during the CLA commissioning Pulse No: 81079. This pulse was aimed at checking the D4 lower limit. The shared area correspond to the region beyond the limit enforced by the CLA.

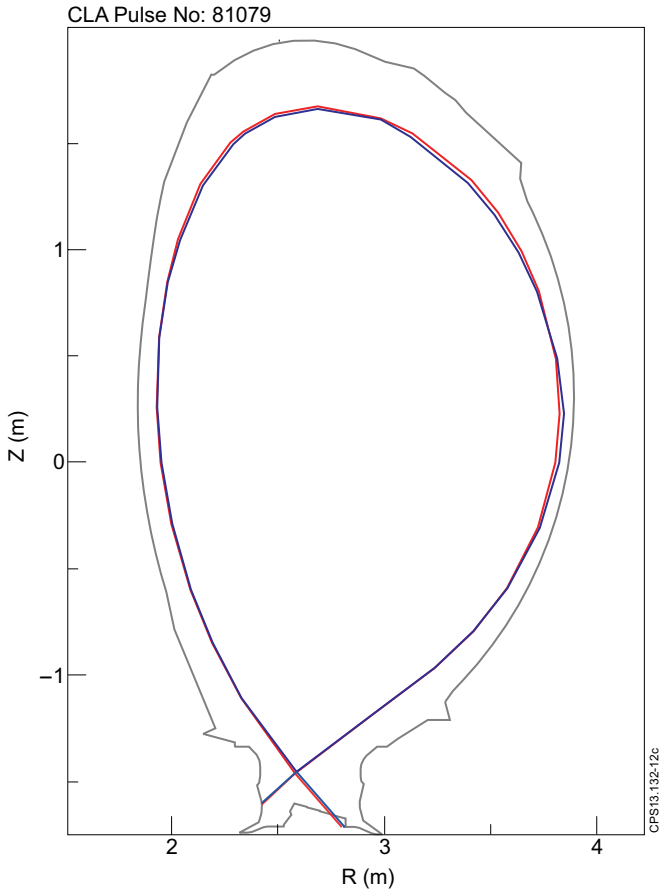

Figure 12: Plasma shape at t = 27s during the CLA commissioning Pulse No: 81079. The red shape is the desired reference while the blue shape is the actual plasma shape at t = 27s.

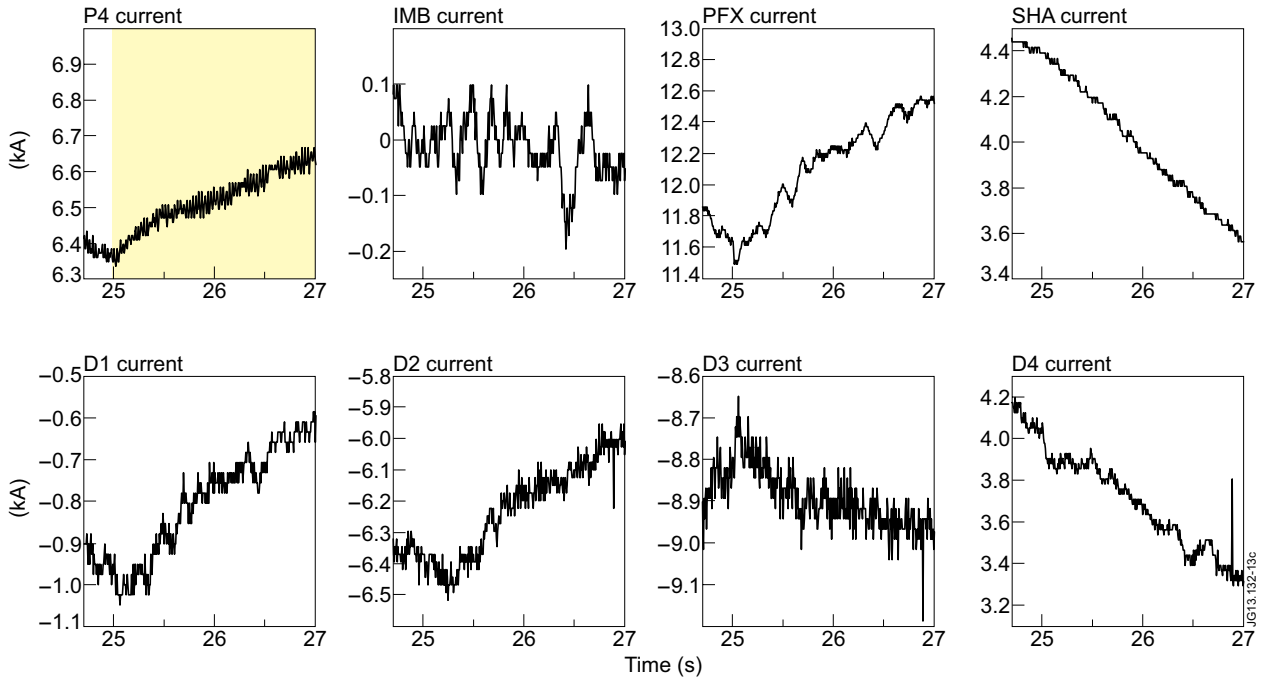

Figure 13: Currents in the PF coils during the CLA commissioning Pulse No: 81081. This pulse was aimed at checking the P4 lower limit. The shared area correspond to the region beyond the limit enforced by the CLA.

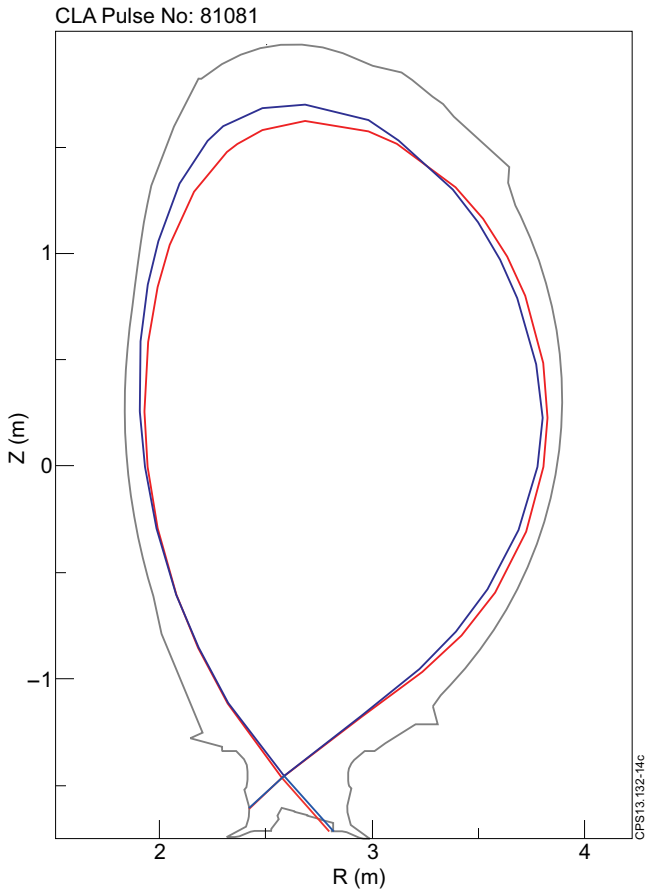

Figure 14: Plasma shape at t = 27s during the CLA commissioning Pulse No: 81081. The red shape is the desired reference while the blue shape is the actual plasma shape at t = 27s; in this case the error due to the CLA is not negligible, hence the CLA does not enforce the current in P4 to the desired value.

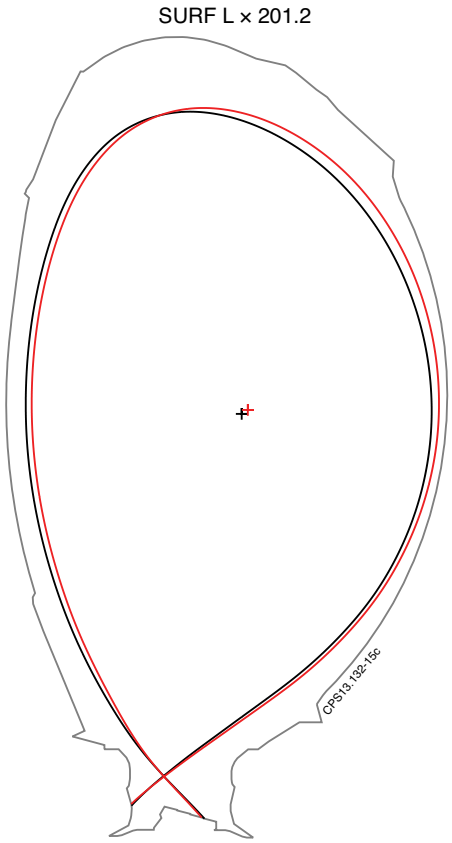

Figure 15: JET Pulse No: 81715. Shape comparison at 22.5s. The black shape is the one obtained in Pulse No: 81710 without CLA, while the red shape is the one obtained when the CLA is enabled.

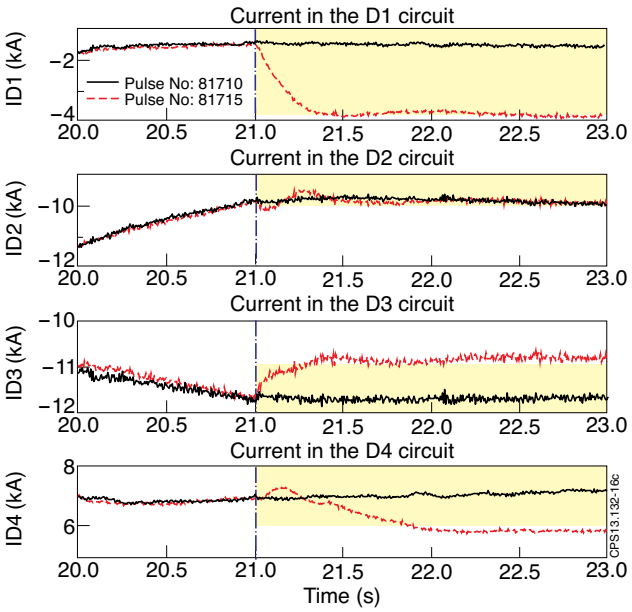

Figure 16: Currents in the divertor circuits. Comparison between Pulse No: 81710 (reference pulse without CLA) and Pulse No: 81715 (with CLA). The shared areas correspond to regions beyond the current limits enforced by the CLA parameters.